

Oscillating Inverted Pendulum and Applications

Ramon Driesen,* Jaden Johnston,† Massimo Pascale,‡ and Evan Ridley§

Department of Mathematics, University of Arizona, Tucson, Arizona, 85719

(Dated: March 20, 2018)

In order for a pendulum to be stable at the upward position, its base needs to be oscillating vertically at a high enough frequency. By studying the stability of an inverted pendulum using different mathematical and physical models, it is possible to find the frequency at which stability occurs when the pendulum is at an upward position. The project focuses on the calculations of the frequency of the oscillations using these well know models, comparing those calculations to the test results, and also introducing the focus of the next phase of the project: studying the stability of a charged pendulum.

I. INTRODUCTION

The vertically oscillating pendulum phenomenon has its roots dating back over a century. Stephenson first published an article describing a potential stability for a pendulum in the upright position given a high frequency oscillation.[1] However, the important step for the mathematical analysis of separating the system into fast and slow systems was not determined until 40 years later by Kapitza.[2]

This separation of fast and slow oscillations makes this system ideal for modeling many other systems. One system of note is the ion trap. By modeling a magnetic pendulum with another magnet underneath its lowest point, two stable equilibrium points are induced. Oscillating the pendulum's base may allow for a model of an ion trap by forcing the pendulum to change which equilibria it rests in. This, like many other applications, requires an understanding of the simple case of a vertically oscillating pendulum. Thus, a full derivation of this case will be covered before delving into other, more complex applications of the same principles.

II. EXPERIMENTAL DETAILS

The experimental process of testing the stability of the oscillating is well documented.[3][4] This testing typically relies on the use of a jigsaw clamped in place to act as an oscillator while a rod acts as a basic pendulum, seen in Fig. 1. By placing this system upright and turning on the jigsaw, a simple experimental model of the vertical oscillating pendulum is produced.

III. MOTION EQUATION

A reformulation of classical mechanics in terms of a variational principle, known as "calculus of variations",

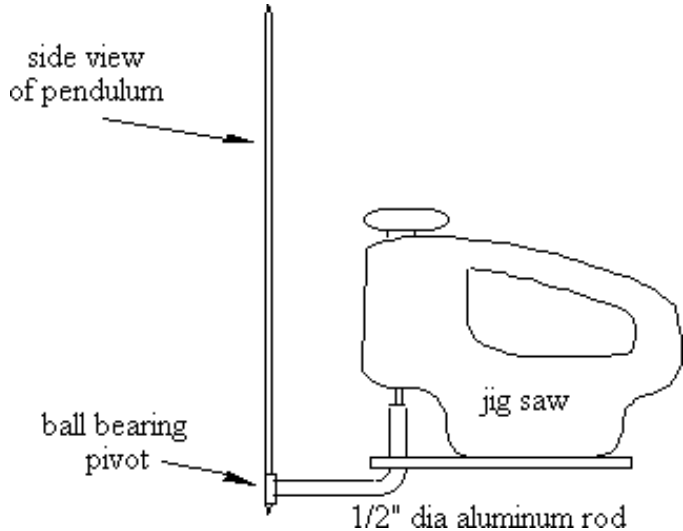


FIG. 1. Pictured is a diagram of the of the inverted pendulum, where the base is oscillated by a jigsaw.[5]

simplifies complicated physical systems. This method is particularly useful when dealing with systems more naturally described by non-Cartesian coordinates like pendulums. The mathematician Lagrange used this variational principle in the late-18th century to re-derive Newtonian mechanics.[6] His method eliminates forces of constraint such as tension while taking the same form in any coordinate system. The derivation in this paper uses this Lagrangian formulation.

The method begins by writing down the kinetic and potential energies of the system, T and U respectively, as in Eq. 1. m is the mass of the object, g is the acceleration due to gravity, x and y are locations, and \dot{x} and \dot{y} are velocities.

$$T = \frac{1}{2}m(\dot{x}^2 + \dot{y}^2) \quad U = mgy \quad (1)$$

In order to calculate these quantities, the system must be defined. Fig. 2 illustrates the system of interest, the vertical pendulum with vibrating base. The image describes the x - and y -positions of the pendulum bob noted in Eq. 2, where the origin is at the lowest point of the

* edriesen@email.arizona.edu

† jadenjohnston@email.arizona.edu

‡ massimopascale@email.arizona.edu

§ evanjridley@email.arizona.edu

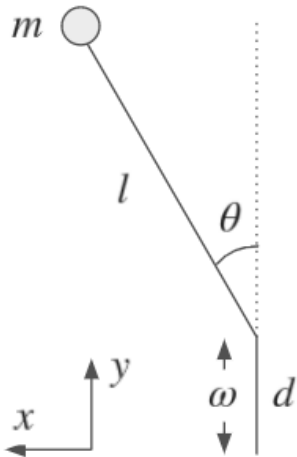


FIG. 2. A base oscillates vertically with angular frequency ω and amplitude d . Atop the base is a pendulum of length l with a bob of mass m . The pendulum is at an angle θ from the vertical axis.

base and θ is a function of time.

$$\begin{aligned} x &= l \sin \theta \\ y &= l \cos \theta + d \cos \omega t \end{aligned} \quad (2)$$

The components of the bob's velocity are the time-derivative of the x- and y-positions, defined by Eq. 3.

$$\begin{aligned} \dot{x} &= l\dot{\theta} \cos \theta \\ \dot{y} &= -l\dot{\theta} \sin \theta - d\omega \sin \omega t \end{aligned} \quad (3)$$

Using Eqs. 2 and 3, the energies in Eq. 1 are evaluated as the following. The trigonometric identity, $\sin^2 \theta + \cos^2 \theta = 1$, simplifies the expression.

$$\begin{aligned} T &= \frac{1}{2}m \left(l^2\dot{\theta}^2 + d^2\omega^2 \sin^2 \omega t + 2ld\omega\dot{\theta} \sin \theta \sin \omega t \right) \\ U &= mg(l \cos \theta + d \cos \omega t) \end{aligned} \quad (4)$$

The Lagrangian, defined in Eq. 5, is proportional to the difference in kinetic and potential energies. This quantity arises from Lagrange's reformulation of mechanics using calculus of variations.[6]

$$L = T - U \quad (5)$$

Using Eq. 4, the Lagrangian in Eq. 5 is evaluated as the following.

$$L = ml \left(\frac{1}{2}l\dot{\theta}^2 + d\omega\dot{\theta} \sin \theta \sin \omega t - g \cos \theta + \frac{1}{2} \frac{d^2\omega^2}{l} \sin^2 \omega t - \frac{gd}{l} \cos \omega t \right) \quad (6)$$

Next, the equation of motion follows in the form of the Euler-Lagrange equation,

$$\frac{d}{dt} \frac{\partial L}{\partial \dot{\theta}} - \frac{\partial L}{\partial \theta} = 0 \quad (7)$$

which is a result of the variational methods.[6] By Eq. 7, an equivalent and simplified Lagrangian which produces the same equation of motion is constructed in Eq. 8, where α is a constant and $f(t)$ is an arbitrary function of time only.

$$L \equiv \alpha (L + f(t)) \quad (8)$$

This states that the equation of motion is invariant under both constant multiplication and additions of total functions of time to the Lagrangian.

The Lagrangian thus simplifies to Eq. 9,

$$L = \frac{1}{2}l\dot{\theta}^2 + d\omega\dot{\theta} \sin \theta \sin \omega t - g \cos \theta \quad (9)$$

and the resulting motion equation is Eq. 10.

$$\ddot{\theta} + \left(\frac{d\omega^2}{l} \cos \omega t - \frac{g}{l} \right) \sin \theta = 0 \quad (10)$$

This differential equation is analyzed to obtain the effective potential.

IV. EFFECTIVE POTENTIAL

The effective potential is the combination of potentials caused by various forces in the system. In the case of the inverted pendulum, forces caused by rapid oscillations of the base as well as the overall slow oscillations of a standard pendulum result in the effective potential. The method of averaging used by Landau and Lifshitz [7] provides an approximation of this potential and involves dissecting the motion into the rapid and slow components aforementioned. The motion then averages over the period of rapid oscillations so that the location of the bob is described by a simple, smooth function. The derivation mimics that seen in VanDalen.[3]

To derive the approximation for the effective potential, the motion of the pendulum, $\theta(t)$, is split into rapid, $\rho(t)$, and slow, $\sigma(t)$, oscillations, as seen in Eq. 11. The rapid oscillations are assumed to be small and average to zero,

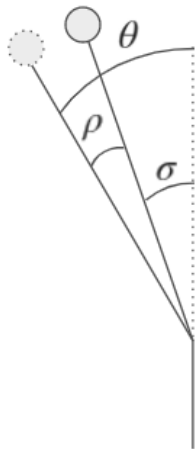


FIG. 3. The pendulum's exact position is at angle θ , the sum of angles ρ and σ , from the vertical axis. The position of the bob oscillates rapidly with displacement ρ about σ . Averaging over small and rapid oscillations, the bob's average position is σ .

as seen in Fig. 3.

$$\theta(t) = \sigma(t) + \rho(t) \quad (11)$$

Additionally, the equation of motion can be rewritten as Eq. 12, to a sum of two functions: F which depends only on θ and f which depends on θ and time.

$$\ddot{\theta} = F(\theta) + f(\theta, t) \quad (12)$$

$$F(\theta) = \frac{g}{l} \sin \theta \quad f(\theta, t) = -\frac{d\omega^2}{l} \cos \omega t \sin \theta$$

Eq. 12 can be Taylor expanded about σ for small values of ρ and then combined with Eq. 11, resulting in an approximation for the motion equation.

$$\ddot{\sigma} + \ddot{\rho} \simeq F(\sigma) + \frac{dF}{d\theta}(\sigma)\rho + f(\sigma, t) + \frac{\partial f}{\partial \theta}(\sigma)\rho \quad (13)$$

By focusing on only rapid oscillations and ignoring oscillations in σ , Eq. 13 simplifies to an equation for $\ddot{\rho}$. Terms with ρ are negligible because $\ddot{\rho}$ is larger than ρ by a factor of ω^2 .

$$\ddot{\rho} \simeq f(\sigma, t) \quad (14)$$

This is a simple ordinary differential equation with the following solution.

$$\rho \simeq \frac{d}{l} \cos \omega t \sin \theta \quad (15)$$

Second, by averaging over the rapid oscillations in Eq. 13, where ρ and $\ddot{\rho}$ average to zero, the motion simplifies to an equation for $\ddot{\sigma}$.

$$\ddot{\sigma} \simeq F(\sigma) + \overline{\frac{\partial f}{\partial \theta}(\sigma)\rho} \quad (16)$$

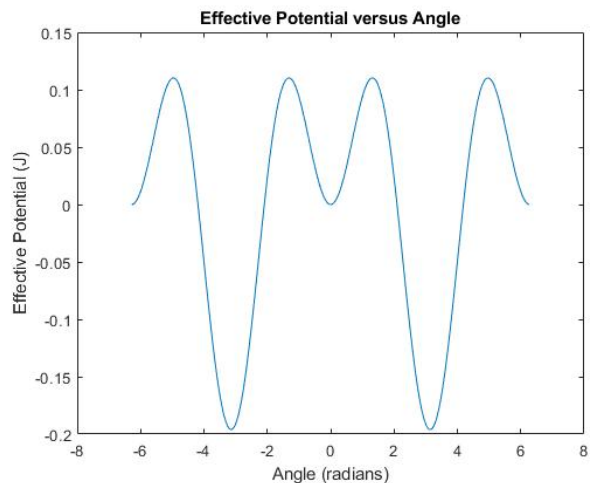


FIG. 4. The amplitude of base oscillations d is 0.05 m. The mass of the pendulum bob m is 10 g. The length of the pendulum l is 1 m. The angular frequency of base oscillations ω is 177 rad/s.

Eq. 16 further simplifies to Eq. 17 after using the integral definition of a function's average value over the period $2\pi/\omega$ and noting that the average value of $\cos^2 \omega t$ equals one-half.

$$\ddot{\sigma} \simeq \frac{g}{l} \sin \sigma - \frac{d^2 \omega^2}{4l^2} \sin 2\sigma \quad (17)$$

Finally, the definition of effective torque is used to find the effective potential. The effective torque on the bob is due to the average movement of the pendulum, given by σ . It is proportional to the bob's moment of inertia I and average angular acceleration $\ddot{\sigma}$ and negatively proportional to the change in effective potential U_{eff} over its average angular motion. These relationships are detailed in Eq. 18

$$I\ddot{\sigma} = -\frac{dU_{eff}}{d\sigma} \quad (18)$$

The moment of inertia of the bob is ml^2 . Rearranging Eq. 18 and integrating results in the effective potential.

$$U_{eff} \simeq mgl \cos \sigma - \frac{md^2 \omega^2}{8} \cos 2\sigma \quad (19)$$

This potential can be analyzed to obtain stability points and frequency limitations. An example of a potential curve is Fig. 4

V. STABILITY

Stability points are defined by local maxima or minima of the effective potential, represented by the following equation.

$$\frac{dU_{eff}}{d\sigma} = 0 \quad (20)$$

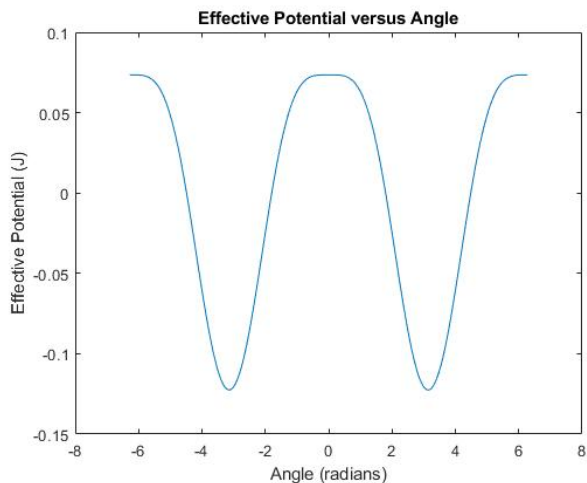


FIG. 5. The amplitude of base oscillations d is 0.05 m. The mass of the pendulum bob m is 10 g. The length of the pendulum l is 1 m. The angular frequency of base oscillations ω is the minimum required for top stability in this scenario, 88.5 rad/s.

Solving Eq. 20 with Eq. 19 results in the following solutions for the critical angles σ_c where n is a real integer.

$$\sigma_c = n\pi, 2n\pi \pm \arccos \frac{2lg}{d^2\omega^2} \quad (21)$$

The first set of critical angles are at the top and bottom of the pendulum while the second set are at arbitrary angles determined by system parameters.

The minimum frequency required to observe top stability occurs when the second set of critical angles are equal to $2n\pi$. This results in the lower bound for the angular frequency of the base ω_l , illustrated in Fig. 5.

$$\omega_l = \frac{\sqrt{2gl}}{d} \quad (22)$$

VI. SIMULATION

Following the derivation of the equation of motion, it is necessary to test the accuracy of the stability analysis. At this stage, it is not yet feasible to test through actual experimentation, so instead it is useful to simulate the findings through numerical analysis.

The equation of motion is similar to that as described in Section III, but with two key differences. Firstly, dampening was added. This effectively removes energy from being a constant of the system, causing center solutions to become spirals. This also visualizes the pendulum getting captured by its stable fixed points, allowing identification of the ‘inverted’ fixed point at the top. Secondly, Eq. 10 is illustrated in terms of \ddot{x}_{base} , and \ddot{y}_{base} ,

which are the Cartesian equations of motion for the pendulum. This was convenient, as it allowed ease of use when changing the pendulum base motion:

$$\ddot{\theta} = \frac{-g \sin(\theta) - \ddot{x}_{base} \cos(\theta) - \ddot{y}_{base} \sin(\theta)}{l} - \alpha \dot{\theta} \quad (23)$$

Here, α represents the dampening constant. For the test of stability of the fixed point at the top of the pendulum, $\ddot{y}_{base} = A \sin(2\pi ft)$ and $\ddot{x} = 0$, where A is the amplitude of base oscillation and f is the frequency of oscillation.

Forward Euler is the method of numerical integration used to solve for θ . [8] For a function $\dot{y}(t) = F(y, t)$, $y(t)$ is found by taking steps forward over a discretized time interval. Defining $y_n \equiv y(t_n)$, the Forward Euler method results in the following.

$$y_{n+1} = y_n + hF(y_n, t_n) \quad (24)$$

Here, h is the time-step. In the context of the simulation, steps are taken forward through $\dot{\theta}$. In other words, $\dot{\theta} = \dot{y}$ in the Forward Euler equation. This is shown by Eq. 25.

$$\dot{\theta}_{n+1} = \dot{\theta}_n + h\ddot{\theta} \quad (25)$$

Where $\ddot{\theta}$ is given by Eq. 10. Using this, $\dot{\theta}$ is calculable. Additionally, using the kinematics equation $\Delta\theta = \dot{\theta}t$ and the time-step h instead of t , it is possible to simultaneously solve for θ .

The simulations show a clear stable fixed point at the top of the pendulum for certain frequencies of pendulum base oscillation. A plot of the θ versus time for a simulation where the pendulum is clearly captured by a this top fixed point can be found in Fig. 6, with the initial parameters listed in the caption. Here, θ converges to ≈ 34.5 radians. This modulo 2π is $\approx \pi$, which corresponds to the top position of the pendulum as θ is defined as the angle from the bottom.

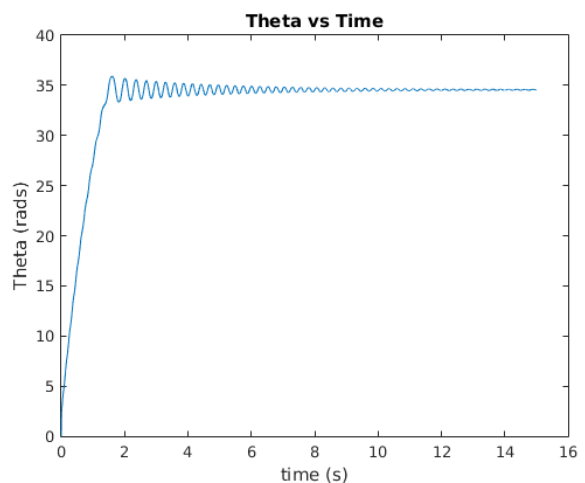


FIG. 6. Plotted is θ versus time for a simulation of the inverted pendulum with initial parameters: $A = 5$ m, $f = 113$ Hz, $h = 0.00013$ s, $l = 1$ m, $\alpha = 0.5$ Hz, $\theta_o = \frac{2}{3}\pi$

VII. PROJECT GOALS

The ion trap is a device that uses electric and magnetic fields to trap charged particles in potential wells. This is incredibly useful for fields like quantum computing, allowing quantum information to be transferred across ions in the same trap.[9] It is possible to make a mechanical analog to the ion trap using pendulums. Should there instead be a charged particle at the end of the pendulum and another charged particle directly below the pendulum, the two potential well system similar to an ion trap can be tested (reference Figure 7 for a visual explanation). The system has three fixed points, where the charges and pendulum are in a straight line and those when the pendulum is on either side of the bottom charge. The former of this is unstable while the latter are stable, and thus the pendulum gets trapped in the potential well on either side of the bottom charge and cannot move between to the unstable fixed point. In the analysis with the vertical pendulum, the oscillations of the base turned a previously unstable fixed point into a stable one. Perhaps the same could be done for the charge pendulum, allowing free movement between traps.

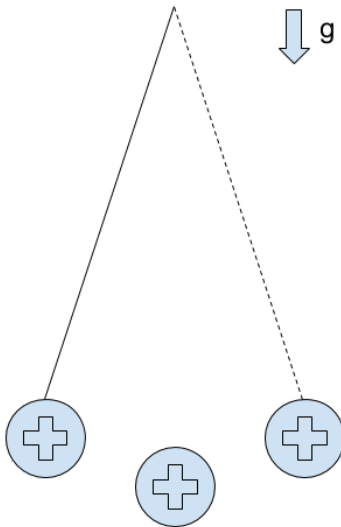


FIG. 7. Pictured is a diagram of the charge pendulum. Here, the large plus signs represents charges. These could easily be replaced with magnets to the same effect.

This could be tested experimentally by using magnets instead of charges. Furthermore, this would act as an analog for the ion trap, perhaps showing this function for a charge pendulum could in turn allow us to apply the same principles for the ion trap. It would be extremely beneficial, as there is not current way of moving between traps in the ion trap.

VIII. PROJECT DETAILS

This charge pendulum project is still in the early stages of development. The projects is expected to have both theoretical and experimental aspects. The former would entail derivation of the equation of motion for the charge pendulum with an oscillating base. Then stability analysis would need to be performed in order to find bifurcations with respect to the frequency of the base and what frequencies cause fixed points to change stability or even appear or disappear. Initial testing of these findings will be done using numerical simulation. This allows testing of multiple scenarios to better design the real world experiment. Jaden and Massimo will be focused on this aspect, while Evan and Ramon will be focusing on the experimental outcome.

Next, these functions must be tested through experimentation. While much of this planning depends on the results of the numerical simulation, a charge pendulum would be created using magnets instead of charges and with the base attached to a jigsaw. Here, the theoretical findings could be tested to translate to real world scenarios.

Once the system has been tested, significance can be extrapolated. This would require extensive research into the ion trap to look for situations analogous to the base oscillation, allowing the principles of the project to transition to that of the ion trap.

IX. ALTERNATIVE PROJECTS

There many other directions that could be explored using this oscillating pendulum analysis. One idea is to use circular motion for the base rather than unilateral. This would amount to setting both x_{base} and y_{base} in Eq. 23 to periodic functions, where the difference in amplitude could cause the motion to be eccentric. Here, the eccentricity could be used as the variable for which dynamics are evaluated to find bifurcations. While this is still not yet analyzed, it is simple to test through numerical simulation explained in Section VI. A simple test was performed using circular motion of the base to motivate further exploration. In both the standard and vertically oscillating cases, there exists fixed points at both the top and bottom positions of the pendulum. As a small check of these base cases, the circular motion pendulum was simulated with an initial angle of the top and bottom positions. It was found that the pendulum moved away from these positions, showing that there are no fixed points at the fully vertical positions, motivating further stability analysis.

X. ACKNOWLEDGEMENTS

The authors would like to thank their professor and mentor, Dr. Ildar Gabitov, for providing guidance and

mentorship. The authors would also like to thank the

University of Arizona for providing the opportunity to perform this project.

-
- [1] A. Stephenson, The London, Edinburgh, and Dublin Philosophical Magazine and Journal of Science **15**, 233 (1908), <https://doi.org/10.1080/14786440809463763>.
- [2] P. L. Kapitza, Soviet Phys. JETP **21**, 588 (1951).
- [3] G. J. VanDalen, (2003), 10.1119/1.1603269.
- [4] N. Povarnitsyna, A. Mkrtchyan, S. Biktimirov, and K. Bronnikov, Skolkovo Institute of Science and Technology (2017).
- [5] “Inverted pendulum demonstration,” <https://sciencedemonstrations.fas.harvard.edu/presentations/inverted-pendulum> (2018).
- [6] J. R. Taylor, *Classical Mechanics* (University Science Books, 2005).
- [7] L. D. Landau and E. M. Lifshitz, *Mechanics*, 2nd ed. (Pergamon, 1969).
- [8] P. R. Bevington and D. K. Robinson, *Data reduction and error analysis for the physical sciences; 3rd ed.* (McGraw-Hill, New York, NY, 2003).
- [9] D. Leibfried, E. Knill, S. Seidelin, J. Britton, R. B. Blakestad, J. Chiaverini, D. B. Hume, W. M. Itano, J. D. Jost, C. Langer, R. Ozeri, R. Reichle, and D. J. Wineland, Nature (London) **438**, 639 (2005).